

Metabolite of SIR2 Reaction Modulates TRPM2 Ion Channel*

Received for publication, December 27, 2005, and in revised form, March 24, 2006 Published, JBC Papers in Press, March 24, 2006, DOI 10.1074/jbc.M513741200

Olivera Grubisha[‡], Louise A. Rafty^{§1}, Christina L. Takanishi^{¶1}, Xiaojie Xu[‡], Lei Tong[‡], Anne-Laure Perraud^{¶1}, Andrew M. Scharenberg^{¶1,2}, and John M. Denu^{‡3}

From the [§]Department of Biochemistry and Molecular Biology, Oregon Health & Science University, Portland, Oregon 97239, the [¶]Department of Pediatrics and Immunology, University of Washington and Children's Hospital and Medical Center, Seattle, Washington 98195, and the [‡]Department of Biomolecular Chemistry, University of Wisconsin, Madison, Wisconsin 53706

The transient receptor potential melastatin-related channel 2 (TRPM2) is a nonselective cation channel, whose prolonged activation by oxidative and nitrative agents leads to cell death. Here, we show that the drug puromycin selectively targets TRPM2-expressing cells, leading to cell death. Our data suggest that the silent information regulator 2 (Sir2 or sirtuin) family of enzymes mediates this susceptibility to cell death. Sirtuins are protein deacetylases that regulate gene expression, apoptosis, metabolism, and aging. These NAD⁺-dependent enzymes catalyze a reaction in which the acetyl group from substrate is transferred to the ADP-ribose portion of NAD⁺ to form deacetylated product, nicotinamide, and the metabolite OAADPr, whose functions remain elusive. Using cell-based assays and RNA interference, we show that puromycin-induced cell death is greatly diminished by nicotinamide (a potent sirtuin inhibitor), and by decreased expression of sirtuins SIRT2 and SIRT3. Furthermore, we demonstrate using channel current recordings and binding assays that OAADPr directly binds to the cytoplasmic domain of TRPM2 and activates the TRPM2 channel. ADP-ribose binds TRPM2 with similarly affinity, whereas NAD⁺ displays almost negligible binding. These studies provide the first evidence for the potential role of sirtuin-generated OAADPr in TRPM2 channel gating.

Transient receptor potential melastatin-related channel 2 (TRPM2)⁴ is a non-selective cation channel mainly expressed in brain, gastrointestinal tissues, and certain immune cells (reviewed in Ref. 1). Although the physiological function of TRPM2 remains unclear, several reports have demonstrated that TRPM2 expression confers susceptibility to cell death in response to oxidative (H₂O₂) and nitrative stress (2, 3). Under these conditions, TRPM2 appears to induce cell death by causing an overwhelming influx of Na²⁺ and Ca²⁺ (2). This influx is thought to occur as a consequence of TRPM2 channel activation via ADP-ribose (ADPr) binding to the cytoplasmic, C-terminal domain of the channel. This domain, termed NudT9-H (NudT9 homology), contains an appar-

ent Nudix enzymatic motif and shares significant homology to the mitochondrial NudT9 enzyme (4, 5), a member of the Nudix ADPr hydrolase family. Indeed, electrophysiology experiments have shown that low micromolar levels of ADPr activate the TRPM2 channel (4, 6), and that this activation is mediated through the NudT9-H domain (7, 8), implicating a direct ADPr and NudT9-H interaction.

The NudT9-H domain has been reported to have hydrolytic activity toward ADPr, albeit at a ~100-fold lower rate than NudT9 (4, 9). Although it was initially thought that the ADPr hydrolase activity of TRPM2 might have a role in regulating TRPM2 gating via hydrolysis of bound ADPr, recent data have demonstrated that mutations in putative catalytic residues of NudT9-H do not affect TRPM2 channel gating, leaving the function of this activity unclear (8). Some studies suggest that hydrogen peroxide directly activates the TRPM2 channel (3, 10); however, it has been reported recently that this oxidative agent acts indirectly by triggering the release of ADPr from an intracellular compartment (8, 11). The mechanism of TRPM2 activation by hydrogen peroxide may prove to be more complex, as hydrogen peroxide and ADPr have also been suggested to act cooperatively in TRPM2 channel activation (12).

In this article, we have investigated the ability of TRPM2 to sensitize cells to cellular insults other than those inducing oxidative stress. Here, we demonstrate that puromycin, a well known pleiotropic cell stress agent, selectively targets TRPM2-expressing cells, leading to cell death. Our studies suggest that Sir2 enzymes play an important role in mediating this response. We found that TRPM2 has the capacity to sense OAADPr, the unique metabolite of the Sir2 protein deacetylase reaction, and induce cell death in response to puromycin. Furthermore, we report the first direct evidence that OAADPr binds to the NudT9-H domain and modulates TRPM2 channel activity. Our data have important implications for the potential physiological roles of ADPr-related molecules as secondary messengers. This report links Sir2 enzymes (sirtuins) with the TRPM2 channel through the Sir2 metabolite OAADPr. This newly discovered association provides a plausible mechanism for previously described sirtuin functions, which include control of stress response pathways and metabolic regulation.

EXPERIMENTAL PROCEDURES

Cell Culture—HEK-293 and tetracycline (tet)-inducible HEK-293 TRPM2-expressing cells (4) were cultured in DMEM and 10% fetal bovine serum at 37 °C, 5% CO₂. Medium used to culture tet-inducible HEK-293 cells was supplemented with blasticidin (5 μg/ml; Invitrogen) and zeocin (0.4 mg/ml; Invitrogen). To induce expression of TRPM2 in recombinant HEK-293 cells, tet was added to the medium at 1 μg ml⁻¹ (Invitrogen) 24 h prior to experiments. The CRI-G1 rat β-islet tumor cell line was obtained from EACC and cultured in DMEM, 10% fetal bovine serum, and 2 mM glutamine.

Cell Viability Assays—HEK-293, tet-inducible HEK-293, and CRI-G1 cells were seeded into 6-well plates at a density of 500,000 cells per

* The costs of publication of this article were defrayed in part by the payment of page charges. This article must therefore be hereby marked "advertisement" in accordance with 18 U.S.C. Section 1734 solely to indicate this fact.

¹ Supported by a C. J. Martin Postdoctoral Research Fellowship 209667 (National Health and Medical Research Council of Australia).

² Supported by National Institutes of Health Grant GM64091.

³ Supported by National Institutes of Health Grant GM65386. To whom correspondence should be addressed: Dept. of Biomolecular Chemistry, University of Wisconsin-Medical School, 1300 University Ave., Madison, WI 53706. Tel.: 608-265-1859; Fax: 608-262-5253; E-mail: jmdenu@wisc.edu.

⁴ The abbreviations used are: TRPM2, transient receptor potential melastatin-related channel 2; Sir2, silent information regulator 2; OAADPr, 2'-O-acetyl-ADP-ribose; ADPr, ADP-ribose; NudT9-H, NudT9 homology; tet, tetracycline; H₂O₂, hydrogen peroxide; PARP-1, poly(ADP-ribose) polymerase 1; PARG, poly(ADP-ribose)glycohydrolase; [³²P]-N₃-ATP, 8-azidoadenosine 5'-[α-³²P] triphosphate; HPLC, high performance liquid chromatography; ITC, isothermal calorimetry; PBS, phosphate-buffered saline; DMEM, Dulbecco's modified Eagle's medium; HEK, human embryonic kidney cells.

Sir2 Modulates TRPM2 Ion Channel

well. When cells were 50–70% confluent, puromycin (Sigma) was added to the medium at various concentrations, and the cells were incubated for 16 h (unless otherwise indicated). Cell monolayers were rinsed with PBS, after which 0.5 ml of 2 μ M calcein (Molecular Probes) in PBS was added directly to the well for 10–20 min. Calcein is retained in living, but not dead cells, where it undergoes catalytic conversion into a fluorescent compound. Fluorescence in each well was measured in a microplate reader using excitation and emission filters at 485/530 nm, respectively.

Calcium Depletion—When TRPM2-expressing HEK-293 cells were 80–90% confluent, they were rinsed with PBS, and incubated in DMEM lacking calcium chloride in the presence of 5 mM EGTA and 1 μ g/ml tet. One hour after calcium removal, cells were treated with 0, 50, 100, 200, or 500 μ M puromycin for 6 h. At this time cells remained adherent and were assayed for viability as described above.

Detection of FLAG-TRPM2 by Western Blot Analysis—HEK-293 TRPM2-expressing cells were grown in the presence or absence of tet (1 μ g/ml) for 24 h. Cells were then rinsed with PBS and lysed directly on the plate with 1 \times protein sample buffer. Whole cell extracts were resolved on a 6% SDS-PAGE gel, and transferred onto a polyvinylidene difluoride membrane. Expression of FLAG-TRPM2 was detected by standard Western blot procedure using a M2 monoclonal anti-FLAG antibody (Sigma).

Knockdown of SIRT2 and SIRT3 Transcription using siRNA—Tet-inducible HEK-293 cells were transfected with 100 nM control, SIRT2 or SIRT3 siRNA (Dharmacon) using Trans-IT TKO transfection reagent (Mirus). After 24 h, TRPM2 expression was induced by addition of tet to the medium. 48-h post-transfection, one set of cells was harvested and analyzed for SIRT expression as described below, and the rest were treated with puromycin for an additional 16 h and assayed for viability.

Analysis of SIRT2 and SIRT3 Transcripts by RT-PCR—Total RNA was isolated from harvested cells using TRIzol reagent (Invitrogen). RNA was reverse-transcribed using random hexamers and AMV-RT (Promega). The RT reaction was used as a template for PCR amplification of SIRT2 or SIRT3 using primer pairs: 5'-CAGAACATAGATACCCTGGAGCGAA and 5'-AAGGTCCTCCAGCTCCTTCTTC and 5'-TGAGAGAGTGTCCGGGCATCCCTG and 5'-TCATCCTATTTGTCTGGTCCATCAA, respectively. Primers 5'-GGCACCACCTTATACAAT and 5'-ATGTCACGCACGATTTC were used to amplify actin, which served as an internal PCR control.

Detection of SIRT2 and SIRT3 Protein by Western Blot Analysis—Cells were lysed in 50 mM Tris-HCl, pH 8.0, 150 mM sodium chloride, 1% Igepal CA-630, 0.5% sodium deoxycholate, 0.1% sodium dodecyl sulfate, 1 mM phenylmethylsulfonyl fluoride, 10 μ g/ml aprotinin, and 10 μ g/ml leupeptin. Cytosolic and mitochondrial fractions were separated using a mitochondrial isolation kit (Pierce) according to the manufacturer's instructions. SIRT2 and SIRT3 protein were detected by standard Western blot protocol using chicken anti-SIRT2 antibody (13) and rabbit anti SIRT3 antisera (14), respectively (antibodies were graciously provided by Dr. Eric Verdin, UCSF).

Synthesis and Purification of OAADPr—As previously described (15–18), OAADPr was generated in a reaction including 50 mM Tris-Cl, pH 7.5, 1.8 mM acetylated histone peptide, 800 μ M NAD⁺, and 40 μ M Hst2 (yeast Sir2 homolog). After 60 min at 37 °C, NADase (Sigma) was added to degrade the remaining NAD⁺. The reaction was quenched 15 min after NADase addition with trifluoroacetic acid (1% final), and OAADPr was separated from other components in the reaction by C18 reverse-phase chromatography (Grace Vydac). Based on HPLC analysis, OAADPr was determined to be >95% pure.

Channel Gating—Patch clamp electrophysiology was performed as previously described (4). Briefly, cells were patch clamped in the whole cell configuration at 25 °C using pipettes with resistances ranging from 2–3 MOhms. Currents were recorded on an EPC9 patch clamp amplifier with automatic capacitance compensation using a protocol generating a 50 ms voltage ramp from –100 to +100 mV every 2 s at a holding potential of 0 mV (appropriately corrected for liquid junction potential). Bath solution included 150 mM NaCl, 2.8 mM KCl, 5 mM CsCl, 1 mM CaCl₂, 2 mM MgCl₂, and 10 mM Hepes, pH 7.2. Pipette solution included 135 mM cesium glutamate, 1 mM MgCl₂, 8 mM NaCl, 10 mM Hepes, pH 7.2, and either no EGTA (unbuffered conditions) or 10 mM EGTA (buffered conditions) as indicated. For low resolution presentation of current development over the course of the experiment, instantaneous currents at –80 mV were extracted from each ramp and plotted *versus* time.

Cloning, Expression, and Purification of the NudT9-H Domain—The DNA sequence encoding residues 1195–1503 of human TRPM2 (long isoform) was amplified by PCR using primers: 5'-AAGCATGCGT-GAGGACGCTG and 5'-ACAAGCTTTCAGTAGTGAGC. The primers introduced an upstream SphI and a downstream HindIII recognition site (underlined) at the termini of the amplified DNA. The PCR product was gel-purified, digested with SphI and HindIII, and cloned into pQE80 (Qiagen) downstream and in-frame with sequence encoding a His₆ tag. The cloned plasmid was then sequenced to ensure no mutations were present. The plasmid was introduced into the BL21(DE3)pLys strain of *Escherichia coli*, and the NudT9-H protein induced by adding isopropyl-1-thio- β -D-galactopyranoside (0.4 mM final) to the culture once A₆₀₀ reached ~0.5. After a 5 h induction at 30 °C, the bacteria were harvested, resuspended in buffer A: 50 mM Tris-Cl, pH 7.6, 300 mM NaCl, 1 mM β -mercaptoethanol, 10 μ g/ml leupeptin, 1 mM phenylmethylsulfonyl fluoride, and lysed by sonication. The NudT9-H protein was purified by affinity chromatography using nickel-Sepharose resin, followed by cation exchange. The final protein preparation was dialyzed in 50 mM Tris-Cl 7.6, pH 7.6, 0.5 mM TCEP, and stored at –80 °C. Protein concentration was determined by Bradford assay (Bio-Rad) using bovine serum albumin as standard.

Isothermal Calorimetry (ITC)—Binding assays were performed on a VP-ITC instrument (MicroCal) at 25 °C. ADPr, AMP, and NAD⁺ (Sigma) were resuspended in the same buffer used to store the NudT9-H protein: 50 mM Tris-Cl pH 7.6, 0.5 mM TCEP, and the ligand concentration was determined spectrophotometrically. NudT9-H protein concentration was 30–35 μ M, whereas ligand concentrations in the injection syringe were 2–4 mM. The data were fitted using the Origin software (Originlab), assuming a 1:1 stoichiometry of binding.

Synthesis and Purification of [³²P]-N₃-OAADPr—[³²P]-N₃-OAADPr was generated through two enzymatic steps. First, [³²P]-N₃-ATP (Affinity Labeling Technologies) and NMN (nicotinamide mononucleotide) were mixed in a 1:3 molar ratio, together with NMNAT (NMN adenylyl transferase). After 1 h at 37 °C, the reaction was quenched in 1% trifluoroacetic acid. [³²P]-N₃-NAD⁺, the product of the reaction, was purified by C18 reverse phase chromatography. [³²P]-N₃-OAADPr was synthesized the same way as described under “Synthesis and Purification of OAADPr” except that [³²P]-N₃-NAD⁺ was used instead of NAD⁺. NAMAT was expressed from a plasmid generously provided by Dr. Mathias Ziegler (Freie Universität Berlin).

[³²P]-N₃-OAADPr photocross-linking—NudT9-H (2 μ M) was incubated in a 300- μ l reaction containing 20 mM Tris-Cl (pH 7.25), 1 mM MgCl₂, [³²P]-N₃-OAADPr (6.5 μ M, ~1 \times 10⁶ cpm), and varying concentrations of cold (unlabeled) OAADPr, ADPr, or NAD⁺. Reactions were incubated at 4 °C for 20 min. In separate control reactions, 2 μ M of bovine serum albumin or heat-denatured NudT9-H (5 min, 95 °C) were

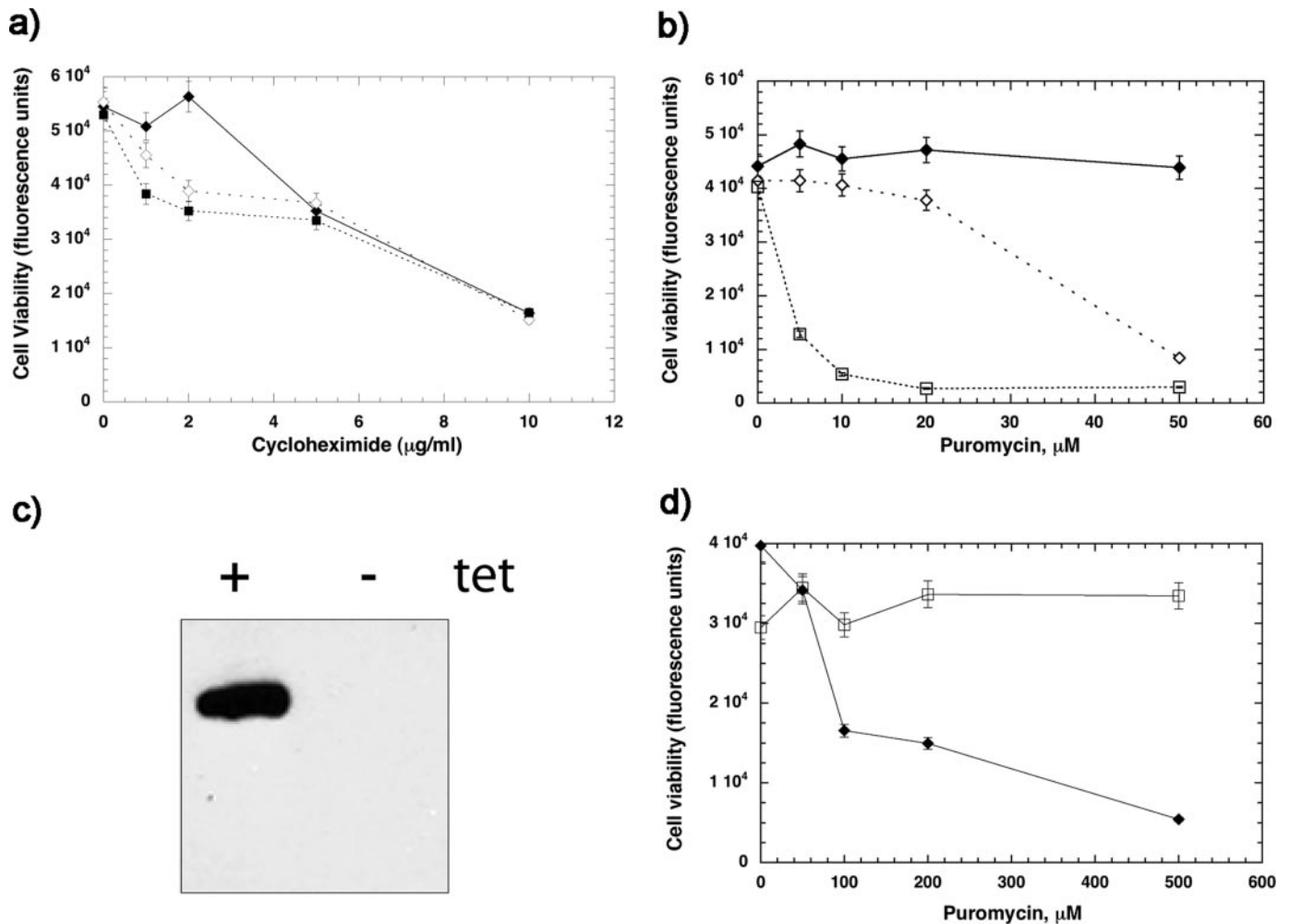


FIGURE 1. *a*, TRPM2 expression in HEK-293 cells does not lead to preferential sensitivity to cycloheximide. HEK-293 (closed diamond) and TRPM2-expressing HEK-293 cells in the absence (open diamond) or presence of (closed square) tet were exposed to 0–10 μg/ml cycloheximide for 16 h. Cell viability was assayed by measuring calcein fluorescence in live, adherent cells. *b*, puromycin leads to cell death in TRPM2-expressing HEK-293 cells. Shown are parental HEK-293 cells (closed diamond) and tet-inducible TRPM2-expressing HEK-293 cells in the presence (open squares) or absence of (open diamonds) tet. Cells incubated in the presence of 0–50 μM puromycin for 16 h were assayed for viability as described above. *c*, FLAG-TRPM2 protein is detected in tet-induced (+) but not non-induced (–) HEK-293 TRPM2 cells. *d*, removal of calcium rescues cells from puromycin-induced cell death. TRPM2-expressing HEK-293 cells were grown in DMEM/10% fetal bovine serum and 1 μg/ml tetracycline until 80–90% confluent. One set of cells was fed with DMEM (closed diamonds), and the other set was fed with DMEM lacking calcium chloride (open squares) in the presence of 5 mM EGTA. One hour after calcium removal, cells were incubated in 0–500 μM puromycin for 6 h after which cell viability was measured as described above.

used instead. Samples were then photolyzed for 8 min using a hand held UV lamp (Mineralight Model UVG-11). Any remaining reactive azido groups were quenched with 10 mM dithiothreitol. Samples were trichloroacetic acid-precipitated, resolved by SDS-PAGE, and visualized by phosphorimaging.

RESULTS

Expression of TRPM2 confers susceptibility to cell death in response to a variety of oxidative and nitrative agents, particularly hydrogen peroxide (2, 3). Given the sensitivity of TRPM2-expressing cells to oxidative stress, we questioned whether other types of chemical affronts could lead to TRPM2 channel activation, and subsequent cell death. We focused our attention on pleiotropic drugs: cycloheximide and puromycin, both of which inhibit protein translation and can lead to apoptosis. We performed a series of cell survival studies following cycloheximide or puromycin treatment of stably transfected HEK-293 cells harboring a tet-inducible *TRPM2* gene. As displayed in Fig. 1*a*, cells expressing TRPM2 did not exhibit increased sensitivity to cycloheximide compared with control cells (non-induced and parental HEK 293 cells). In contrast, tet-induced TRPM2-expressing cells displayed a profound

sensitivity to puromycin-dependent cell death with as little as 5 μM puromycin (Fig. 1*b*). The dose response curve, displayed a strong dependence up to 50 μM puromycin. In the absence of TRPM2 expression (Fig. 1*c*), cells exhibited nearly complete protection against puromycin-dependent cell death (Fig. 1*b*). Parental HEK-293 cells showed no significant cell death following puromycin treatment (5–50 μM) in the absence (Fig. 1*b*) or presence of tet (data not shown). These data indicate that TRPM2 expression renders cells more susceptible to puromycin, but not cycloheximide, mediated cell death, and suggest that inhibition of protein synthesis alone is insufficient to cause cell death via activation of the TRPM2 channel.

Full activation of the TRPM2 channel is dependent on extracellular Ca²⁺ (2, 19–21), thus, we examined whether puromycin-induced cell death in TRPM2-expressing cells required the presence of extracellular Ca²⁺. Because prolonged incubation in Ca²⁺-free medium in itself leads to cell death over time, we assayed cell viability in Ca²⁺-free medium at 6 h rather than 16-h post-drug treatment, and adjusted the range of puromycin concentration accordingly to 100–600 μM. The removal of Ca²⁺ 1 h prior to drug treatment completely blocked puromycin-induced cell death in TRPM2-expressing cells (Fig. 1*d*). These results dem-

Sir2 Modulates TRPM2 Ion Channel

onstrate that the observed puromycin-induced cell death is dependent on Ca^{2+} and, provides additional support for puromycin activation of the TRPM2 channel.

The above results suggest that puromycin causes sustained TRPM2 channel activation in HEK-293 cells, by means other than protein synthesis inhibition, leading to cell death. We hypothesized that the molecular link between puromycin and TRPM2 channel gating may be activation of poly(ADP-ribose) polymerase 1 (PARP-1). As a precursor to apoptosis, PARP-1 is activated in response to cellular signals and DNA damage (reviewed in Ref. 22). This nuclear enzyme synthesizes poly(ADP-ribose) from NAD^+ and attaches the polyADP-ribosyl moiety onto multiple protein targets. Poly(ADP-ribose) can be rapidly hydrolyzed by PARG (poly(ADP-ribose) glycohydrolase) to form ADP-ribose, which could then activate the TRPM2 channel. We investigated whether PARP inhibitors 3-aminobenzamide and nicotinamide could protect TRPM2-expressing cells from puromycin-induced cell death. Curiously, 3-aminobenzamide, a potent PARP inhibitor displaying an IC_{50} of $\sim 5 \mu\text{M}$ *in vivo* (23), had no effect on puromycin-induced cell death even at 1.5 mM (Fig. 2a). In contrast, nicotinamide (500 μM) completely protected puromycin-induced cell death up to concentrations as high as 20 μM puromycin (Fig. 2b). Only at a much higher puromycin concentration (50 μM) could the protection afforded by nicotinamide be suppressed. *In vivo*, nicotinamide inhibits PARP-1 at an IC_{50} of 100 μM (23), and is therefore a considerably weaker PARP-1 inhibitor than 3-aminobenzamide. These results suggested that nicotinamide protection from puromycin-induced cell death occurs through a mechanism distinct from PARP inhibition.

We hypothesized that nicotinamide could be inhibiting a different class of NAD^+ -dependent enzymes, in particular, the Sir2 family of histone/protein deacetylases. Members of this family have been shown to regulate numerous cellular functions including: gene expression, apoptosis, metabolism, differentiation, and aging (reviewed in Ref. 24). Seven homologues of the prototypic yeast Sir2 enzyme have been identified in mammalian cells (SIRT1–7) (25, 26), and nicotinamide, a product of the Sir2 deacetylation reaction, is a potent inhibitor of Sir2 enzymes, displaying IC_{50} values in the low micromolar range (27–29). We examined whether two likely candidates, cytoplasmic SIRT2 and mitochondrial SIRT3, could mediate the puromycin-induced TRPM2 channel gating. RNA interference (siRNA) was used to knockdown the endogenous mRNA and protein levels, and the resulting effect on puromycin-induced cell death was assessed (Fig. 3). In these experiments, a nonspecific siRNA control and siRNA specific for SIRT2 and SIRT3 were used. As shown in Fig. 3a, each siRNA demonstrated strict specificity, only knocking down its corresponding RNA and protein, whereas having no effect on the other. After siRNA treatment, endogenous levels of SIRT3 protein in whole cell extracts could no longer be detected. Similar knockdown was seen with SIRT2 siRNA treatment. Data shown in Fig. 3b represent averages obtained from five separate experiments (including standard deviations) with five different concentrations of puromycin. Relative to nonspecific siRNA transfection, cells transfected with either SIRT2 or SIRT3 siRNAs displayed significant resistance to puromycin-induced cell death in TRPM2-expressing HEK-293 cells (Fig. 3b). At 20 μM puromycin, loss of SIRT2 or SIRT3 increased cell survival 2–3-fold, and by 50 μM puromycin, $\sim 30\%$ of the original cell number was still viable, whereas survival of control siRNA-treated cells was negligible.

The above results showed that depletion of SIRT2 or SIRT3 confers protection from puromycin death in TRPM2-expressing cells. Because these two enzymes reside in different cellular regions, it is unlikely that they deacetylate the same substrates. However, both enzymes catalyze

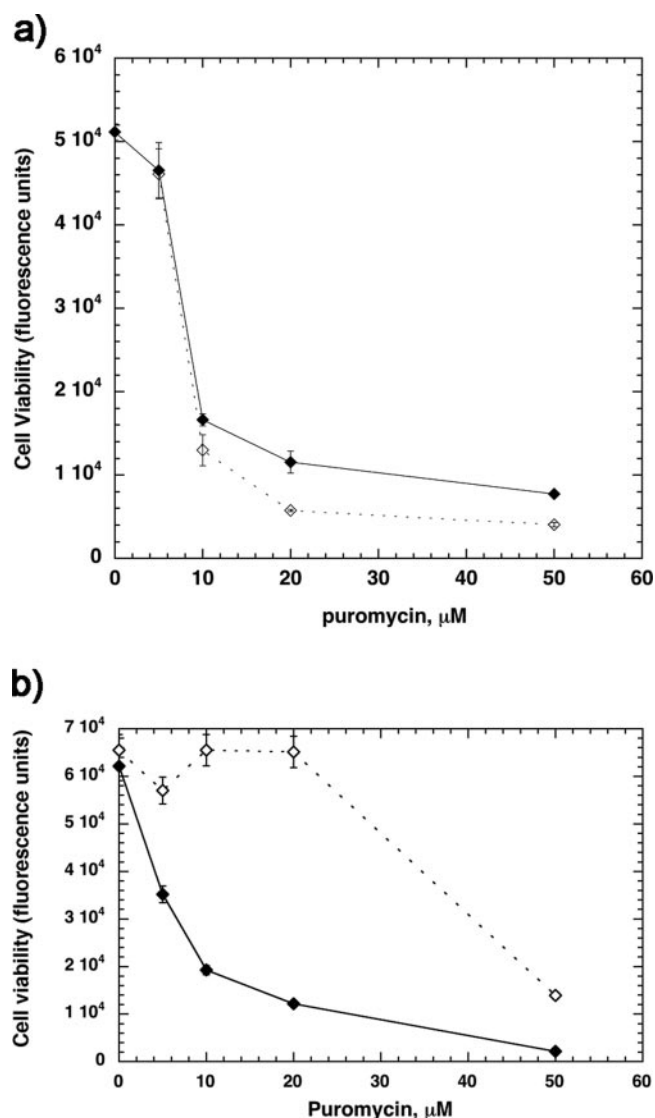


FIGURE 2. *a*, PARP inhibitor 3-amino-benzamide does not block puromycin-induced cell death. TRPM2-expressing HEK-293 cells were exposed to 0–50 μM puromycin for 16 h in the presence (*open diamond*) or absence (*closed diamond*) of 1.5 mM 3-aminobenzamide. Cell survival was determined by measuring fluorescence of calcein in live, adherent cells. Results (with standard deviations) are representative of two or more independent experiments. *b*, nicotinamide blocks puromycin-induced cell death in TRPM2-expressing cells. TRPM2-expressing HEK-293 cells were exposed to 0–50 μM puromycin for 16 h in the presence (*open diamond*) or absence (*closed diamond*) of 500 μM nicotinamide. Cell viability was then measured as described above.

an NAD^+ -dependent reaction in which the acetyl group is transferred to the ADP-ribose portion of NAD^+ to generate the metabolite OAADPr (15, 17, 30, 31). We postulated that OAADPr, the product of the Sir2 reaction, might accumulate during puromycin treatment and cause TRPM2 channel activation. Given the structural similarity of OAADPr to ADPr, we hypothesized that OAADPr may be responsible for directly gating the TRPM2 channel. To test this hypothesis, we performed whole cell patch clamp experiments in TRPM2-expressing HEK-293 cells. We found that inclusion of OAADPr in the patch pipette solution induced currents in TRPM2-expressing cells (Fig. 4b), but not when TRPM2 was absent (Fig. 4c). OAADPr activated these with similar kinetics and dose dependence to that of ADPr (compare Fig. 4, *a* and *b*, *top panels*). These currents were characteristic of TRPM2 as they were absent when TRPM2 expression was absent (Fig. 4c), exhibited a linear I/V relationship characteristic to TRPM2 (Fig. 4, *a* and *b*, *bottom pan-*

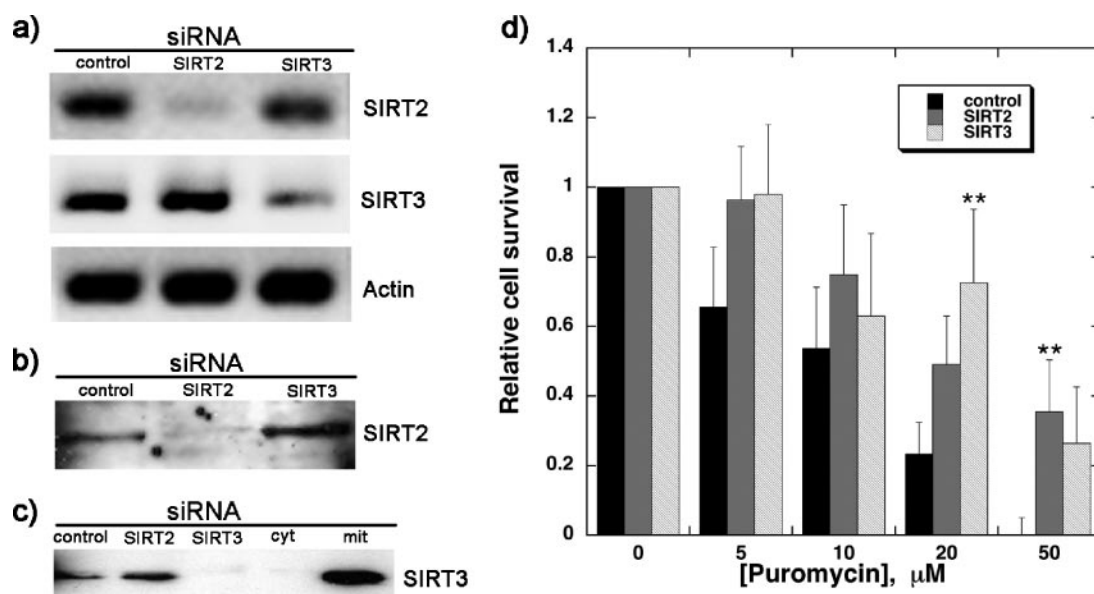


FIGURE 3. *a–c*, detection of SIRT2 and SIRT3 mRNA and protein levels in siRNA-treated TRPM2-expressing HEK-293 cells. Cells treated for 48 h with 100 nM control, SIRT2, or SIRT3 siRNA were harvested and analyzed for knock-down in SIRT2 and SIRT3 expression. *a*, presence of SIRT2 and SIRT3 transcripts was detected by RT-PCR. The amount of total RNA used for RT-PCR was normalized to that of actin. *b*, endogenous SIRT2 protein levels were detected by Western blot using anti-SIRT2 antibody. *c*, SIRT3 protein, detected by Western blot using anti-SIRT3 antisera, was detected in the mitochondrial but not the cytosolic fraction. *d*, siRNA knock-down of endogenous SIRT2 and SIRT3 protein protects cells against puromycin-induced death. TRPM2-expressing HEK-293 cells were transfected with 100 nM nonspecific control, SIRT2, or SIRT3 siRNA. After 48 h, cells were exposed to 0–50 μM puromycin for an additional 16 h. Cell survival was determined by measuring fluorescence of calcein in live cells, and plotted as a fraction relative to the no puromycin control. Results are averages (with standard errors) from six separate experiments. **, indicates $p < 0.05$ from analysis of variance statistical analysis, comparing siRNA control data with that of SIRT2 or SIRT3 at each puromycin concentration.

els), and were potentiated when intracellular Ca^{2+} was left unbuffered (Fig. 4*d*). After performing the above experiments, we determined that spontaneous breakdown of OAADPr to ADPr in the patch pipette was <5 –10%. As this level of breakdown would not allow for sufficient accumulation of ADPr to induced channel gating, these data are consistent with OAADPr, and not the breakdown product ADPr, acting as the direct ligand in the recordings. The similarity of the dose response relationship for OAADPr-mediated gating of TRPM2 to that for ADPr-mediated gating of TRPM2 further suggests that OAADPr activates the TRPM2 channel as effectively as ADPr, and may indeed serve as a physiological regulator of TRPM2.

To verify that puromycin does not directly gate the TRPM2 channel, whole cell channel recordings were performed with 100 μM puromycin alone, which showed no effect on channel activity (data not shown). Also, there was no significant enhancement of OAADPr-gated TRPM2 channel activity in whole cell recordings when 125–250 μM puromycin was included in the patch pipette (Fig. 4*e*). These data demonstrate that puromycin does not directly gate the TRPM2 channel, nor does it modulate TRPM2 gating properties in response to OAADPr. Therefore, puromycin is indirectly responsible for TRPM2-dependent cell death, possibly by mediating OAADPr accumulation. The mechanism by which puromycin leads to increased levels of OAADPr is unclear; however puromycin might increase sirtuin activity or inhibit the breakdown pathways of OAADPr.

We sought to substantiate our observations of OAADPr-gated TRPM2 activity using a genetically unmodified cell line. TRPM2 is highly expressed in rat microglia (32), and has been described in granulocytes (4, 6, 33), rat insulinoma cell lines (2, 20, 34), and pancreatic β -islets (35). We chose to conduct experiments on CRI-G1 (rat β -islet insulinoma) cells, in which the endogenous TRPM2 channel has been well characterized (11, 20, 34, 36–38). Puromycin treatment of CRI-G1 cells led to dose-dependent cell death at the same range of puromycin concentrations as those used in the TRPM2-inducible HEK-293 system (Fig. 5*a*). In addition, the Sir2 inhibitor nicotinamide was able to protect

cells from puromycin-induced death in a dose-dependent manner (Fig. 5*a*, inset), whereas the PARP inhibitor 3-aminobenzamide showed no protective effect (data not shown). Most importantly, OAADPr was able to directly mediate gating of currents in CRI-G1 cells, which exhibited the characteristic TRPM2 I/V relationship (Fig. 5*b*, bottom panel). Inclusion of OAADPr in the patch pipette produced evolution of average currents of 2 nA with a highly linear I/V relationship characteristic of TRPM2. No current evolution was detected in the absence of OAADPr (light gray curve, Fig. 5*b*), whereas the evolution of the OAADPr-induced currents occurred over a time course consistent with diffusional equilibration of OAADPr into the cell from the patch pipette. Overall, these results support the physiologic relevance of OAADPr in regulating TRPM2 channel gating.

We next asked whether OAADPr activates the channel via direct binding to the NudT9-H domain. This domain may regulate TRPM2 channel gating by differentially binding to small, adenosine-containing ligands, such as NAD^+ , ADPr, OAADPr, and AMP. However, no report had demonstrated direct, biologically relevant binding to this domain. To examine whether these molecules directly bind to NudT9-H, we performed ITC binding experiments using recombinant purified NudT9-H from TRPM2. Whereas no NAD^+ binding was observed up to the limit of detection (250 μM), ADPr bound NudT9-H with a K_d of 130 μM (Fig. 6*a*), in agreement with the observed EC_{50} for ADPr-mediated TRPM2 gating (4). AMP also bound NudT9-H, albeit at a lower affinity than ADPr ($K_d = 166 \mu\text{M}$) (data not shown), consistent with a recent report demonstrating that AMP inhibits ADPr-mediated TRPM2 channel activation, displaying an IC_{50} of $\sim 70 \mu\text{M}$ (12). Unfortunately, because of high concentrations of ligand required for the ITC experiments, we were unable to generate sufficient quantities of OAADPr for ITC analysis. We, therefore, used a UV-cross-linking approach to examine OAADPr binding to NudT9-H. We generated [^{32}P]- N_3 -OAADPr, a [^{32}P]-labeled OAADPr compound with an UV reactive azido (N_3) group attached to the adenine ring. [^{32}P]- N_3 -OAADPr was incubated with NudT9-H in the absence or presence of

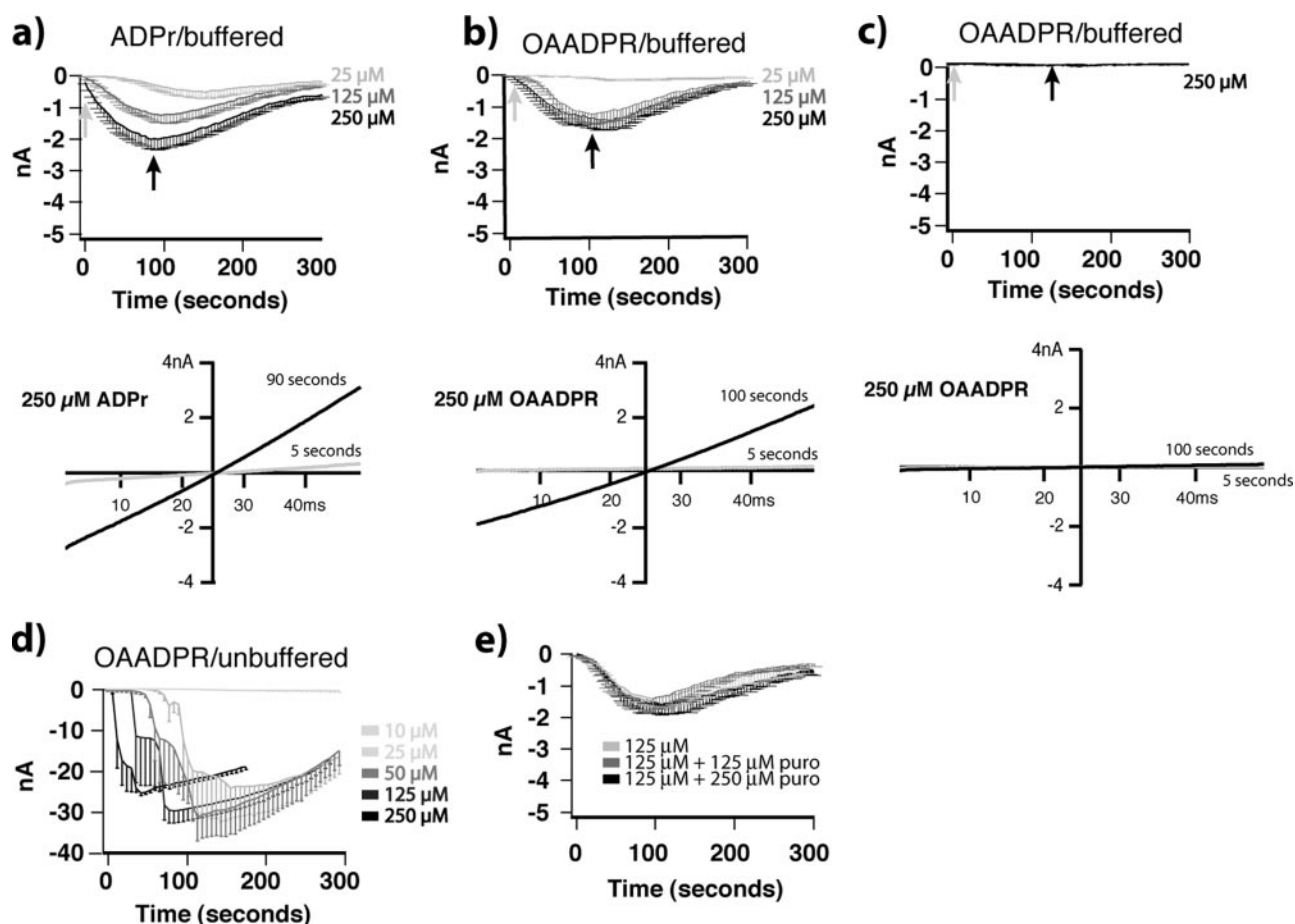


FIGURE 4. **The TRPM2 channel is gated by OAADPr in HEK-293 cells.** *a–c*, top panels illustrate the development of whole cell currents over time in TRPM2-expressing HEK-293 cells; bottom panels show I/V relationships of currents shortly after break in, and at peak current development. Bath solution was standard Ringer's, and pipette solution was Cs-based and included 10 mM EGTA and the indicated concentrations of ADPr or OAADPr. *a*, HEK cells induced to express TRPM2 with ADPr-containing pipette solutions; *b*, HEK cells induced to express TRPM2 with OAADPr-containing pipette solutions; *c*, non-induced HEK cells with 250 μM OAADPr containing pipette solution. *d*, development of whole cell currents in HEK cells induced to express TRPM2 with OAADPr-containing pipette solutions lacking EGTA. *e*, development of whole cell currents in HEK cells induced to express TRPM2 with pipette solutions containing OAADPr (125 μM) and puromycin as indicated.

increasing concentrations of unlabeled OAADPr, ADPr, or NAD⁺ competitor. As shown in Fig. 6b, [³²P]-N₃-OAADPr readily cross-linked with NudT9-H. No radiolabel was incorporated when heat-denatured NudT9-H or BSA were used in parallel controls experiments (data not shown), indicating that [³²P]-N₃-OAADPr specifically binds to a structured component of the NudT9-H domain. Increasing amounts of either cold OAADPr or ADPr efficiently competed away the [³²P]-N₃-OAADPr from the binding site on NudT9-H, suggesting that ADPr and OAADPr bind to the same pocket (Fig. 6b). Quantitation of the signal intensities, plotted in Fig. 6c, shows that both OAADPr and ADPr bind to NudT9-H with similar affinity (~90–100 μM *K_d*), in good agreement with values from the ITC experiments. On the other hand, NAD⁺ did not efficiently compete for binding, since a 100-fold molar excess of NAD⁺ decreased the radiolabel signal intensity by 54% (data not shown). This small decrease can be partially attributed to the amount of contaminating ADPr (estimated to be ~3% by HPLC analysis), which is typical of commercial NAD⁺ preparations. Taking this into account, we estimate that NAD⁺ binds NudT9-H with a ≥20-fold lower affinity than ADPr or OAADPr. These data provide the first evidence of direct OAADPr, ADPr, and AMP binding to the NudT9-H domain, and provide new insight into the regulation of the TRPM2 channel.

DISCUSSION

In this study, we explored the ability of TRPM2 to sensitize cells to metabolic perturbations other than those that induce oxidative stress.

Using cell viability assays, we found that the drug puromycin confers high susceptibility to death in TRPM2-expressing cells, through a mechanism distinct from inhibition of protein translation. We further show that nicotinamide effectively protects cells from puromycin-induced death, and that this protection is consistent with inhibition of the Sir2 family of NAD⁺-dependent protein deacetylases. Specifically, siRNA experiments revealed that depletion of either cytoplasmic SIRT2 or mitochondrial SIRT3 protein results in protection from puromycin death in TRPM2-expressing cells. A common feature of Sir2 enzymes is the generation of OAADPr through an NAD⁺-dependent protein deacetylation reaction. We postulated that SIRT2 and SIRT3 might contribute to the accumulation of cellular OAADPr, leading to TRPM2-dependent cell death. Indeed, we found that OAADPr activates the TRPM2 channel with similar kinetics and dose dependence to that of ADPr, a postulated ligand of TRPM2. Most significantly, we demonstrate using UV cross-linking experiments that OAADPr directly binds the NudT9-H domain of the channel. These data are consistent with the idea that OAADPr produced by SIRT2 and SIRT3 is responsible for the TRPM2 activation and provide compelling evidence that OAADPr is a regulator of TRPM2.

No detectable binding of NAD⁺ to the NudT9-H domain (up to 250 μM) was observed by ITC, whereas ADPr bound with a *K_d* of ~130 μM. UV-cross-linking experiments revealed that NAD⁺ weakly competes with OAADPr for NudT9-H binding, with ≥20-fold lower efficiency

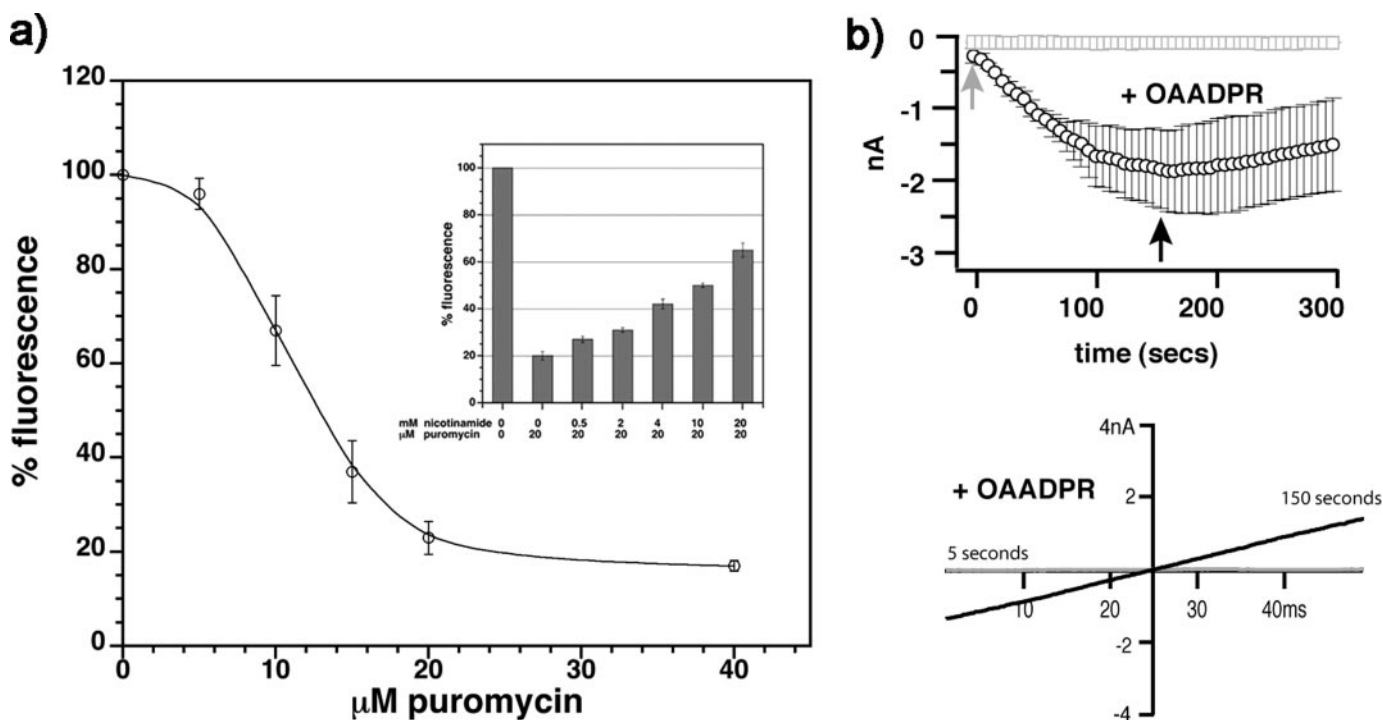


FIGURE 5. *a*, puromycin leads to cell death in CRI-G1 cells. CRI-G1 cells were treated with 0–40 μM puromycin for 16 h. Cell viability was measured by detecting calcein fluorescence in live, adherent cells. Data obtained from four independent experiments were plotted as a percent change in fluorescence compared with those of untreated cells set at a 100%. Error bars indicate the standard deviation from the mean. *Inset*, nicotinamide rescues puromycin-induced death in CRI-G1 cells. CRI-G1 monolayers were treated with 0, 0.5, 2, 4, 10, or 20 mM nicotinamide. After 30 min, puromycin was added to the medium at a final concentration of 20 μM . Cell viability was assessed 16 h later as described above. Data are representative of two independent experiments performed in duplicate. *b*, OAADPr gates the endogenous TRPM2 channel in CRI-G1 cells. *Top panel*, evolution of currents in CRI-G1 cells in the absence (gray squares) or presence (black circles) of OAADPr (120–250 μM). Shown are average leak-subtracted currents from $n = 3$ cells for each condition. *Bottom panel*, representative leak-subtracted whole cell I/V curves for peak currents observed in the absence (gray line) and presence (black line) of OAADPr. For the above measurements, CRI-G1 cells were maintained in the whole cell patch clamp configuration as previously described for HEK-293 cells (4).

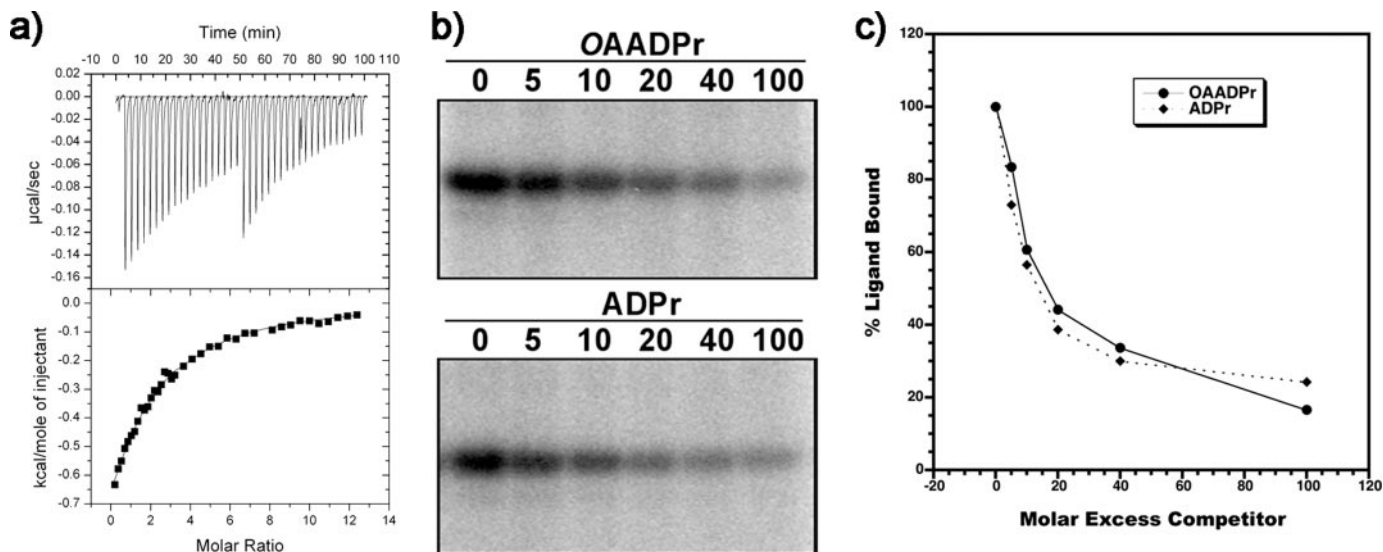


FIGURE 6. *a*, NudT9-H domain binds ADPr. *Top panel*, shown is the isothermal titration calorimetry profile for ADPr binding to NudT9-H. The first, small injection was not used for data fitting. The subsequent nineteen data points were obtained with 4- μl injections of 2 mM ligand, followed by twenty 10- μl injections. *Bottom panel*, data were fitted to an equilibrium binding isotherm. The stoichiometry of binding (N) was set to 1. The K_d for the binding of ADPr to NudT9-H was determined to be $130 \pm 3 \mu\text{M}$. *b* and *c*, the NudT9-H domain binds OAADPr with similar affinity as ADPr. Binding was performed using 2 μM NudT9-H, 6.5 μM [^{32}P]-N₃-OAADPr, and 0, 5, 10, 20, 40, or 100 molar excess cold OAADPr or ADPr competitor. Reactions were incubated for 20 min at 4 °C prior to UV cross-linking. Results were obtained by phosphorimaging (*b*), and the signal intensity was quantitated and plotted as the molar excess of cold competitor versus percent [^{32}P]-N₃-OAADPr bound (*c*).

than ADPr. These data support the view that TRPM2 activation by direct NAD⁺ interaction is unlikely, but rather, occurs after NAD⁺ breakdown. The NudT9-H domain of the channel was reported to have some hydrolytic activity toward ADPr (4, 9). However, recent data demonstrated that mutations in putative catalytic residues of NudT9-H do not affect channel gating (8). In our purified preparations of the NudT9-H

domain, we detected no NudT9-H enzyme activity under our sensitive assay conditions (data not shown) (16), even though direct binding of several ligands to NudT9-H was observed, precluding the possibility of misfolded protein. These results provide strong additional evidence that any intrinsic activity of the TRPM2 NudT9-H is not likely to be a significant regulator of channel function. Intriguingly, we found that AMP,

Sir2 Modulates TRPM2 Ion Channel

an antagonist of the TRPM2 channel (12), exhibited significant capacity to bind NudT9-H ($K_d = 166 \mu\text{M}$). Interestingly, the ratio of AMP to ATP is a well known gauge of cellular energy status (Ref. 39 and references therein). The possibility that the ratio of AMP/(ADPr+OAAADPr) may play an analogous role in TRPM2 function is an intriguing idea to postulate. Sirtuin function is often associated with improved cellular health and better utilization of available energy (40, 41). Under such conditions, increased sirtuin activity and thus accumulation of OAAADPr may decrease the AMP/OAAADPr and stimulate TRPM2 activity.

Studies have linked Sir2 enzymes to diverse functions, in particular, the regulation of cell survival under stress (42–47). Human SIRT1, the best studied yeast Sir2 orthologue, localizes to the nucleus where it deacetylates a number of key proteins, including p53 (47–49), and Foxo transcription factors (42, 44, 50, 51). Tissue-specific functions of SIRT1 include skeletal muscle differentiation (52), fat mobilization in adipocytes (53), gluconeogenesis in the liver during fasting (54), and enhanced glucose-stimulated insulin secretion (55). Less is known about other human Sir2 members. SIRT2 is associated with microtubules in the cytoplasm and can deacetylate α -tubulin (13). The mitochondrial SIRT3 enzyme has been linked to longevity (56, 57), and the regulation of thermogenesis in brown adipocytes (58).

There have been few reports investigating the biological function(s) of OAAADPr and its possible connection with the observed Sir2-dependent biology. It has been suggested that OAAADPr might be a substrate for other linked enzymatic processes, an allosteric regulator, or a second messenger. The first report of bioactivity came from the observation that OAAADPr injected into starfish oocytes or blastomeres caused a block/delay in maturation and cell division, respectively (18). Other roles, such as gene silencing, have been recently ascribed to OAAADPr based on *in vitro* experiments showing OAAADPr binding to macroH2A1.1, a histone variant found in heterochromatic regions (59), and to the Sir2/3/4 silencing complex in yeast (60). Enzymes capable of metabolizing OAAADPr have been detected in several diverse cells (16). *In vitro*, select members of the Nudix family of ADPr hydrolases (e.g. mNudT5 and yeast YSA1) are capable of efficient hydrolysis of OAAADPr, whereas others like human Nudt9 are not (16).

In this study we have provided the first evidence that ADPr and OAAADPr bind the NudT9-H portion of the channel. It is likely that both ADPr and OAAADPr are physiologically important regulators of TRPM2, but that they are generated from diverse cellular stimuli and/or different pathways. For example, OAAADPr may accumulate in response to puromycin cell stress, whereas ADPr might accumulate after hydrogen peroxide treatment, as previously suggested (8, 11). Analogous to a recent report implicating mitochondria as the source of cytoplasmic ADPr, which led to TRPM2 channel activation (8), we hypothesize that OAAADPr generated by SIRT3 is released from the mitochondria during puromycin treatment. In the case of SIRT2, protein deacetylation in the cytoplasm would lead to direct intracellular accumulation of OAAADPr. However, we cannot dismiss the possibility that OAAADPr is converted to ADPr by an esterase activity found in the cytoplasm (16), and that this newly generated ADPr activates the TRPM2 channel. Because the enzymatic source of ADPr in the mitochondria and the mechanism of mitochondrial ADPr release are not known, it is possible that Sir2-generated OAAADPr is the source of mitochondrial ADPr.

Here, we provide the first evidence that OAAADPr, the product of the Sir2 reaction, can modulate cellular responses by regulating the opening of the TRPM2 Ca^{2+} -permeable channel. Although acute accumulation of OAAADPr in our cell-based system may cause susceptibility to cell death, these data suggest that at lower levels of OAAADPr, Sir2-like

enzymes could modulate diverse cellular events by mediating cellular Ca^{2+} entry. Nonselective cation channels, like TRPM2, may play a role in insulin secretion by regulating pancreatic β -cell plasma membrane potential, Ca^{2+} levels, and thus glucose signaling and homeostasis (34). Interestingly, TRPM2 is expressed in β islets, and we have shown that OAAADPr activates TRPM2 in a rat insulinoma cell line. TRPM2 channels and their activation by OAAADPr-producing Sir2 enzymes may provide a mechanism for depolarization or Ca^{2+} entry in insulin producing β -cells, which could lead to the control of insulin secretion and overall glucose homeostasis. Intriguingly, a recent study showed that overexpression of SIRT1 in β -pancreatic islets of transgenic mice resulted in improved glucose tolerance and enhanced glucose-stimulated insulin secretion (55). OAAADPr adds to the list of NAD^+ -derived second messengers (including ADPr, cyclic-ADPr and NAAD(P)) that regulate Ca^{2+} signaling/release, and mediate cell survival (61).

REFERENCES

1. Perraud, A. L., Schmitz, C., and Scharenberg, A. M. (2003) *Cell Calcium* **33**, 519–531
2. Hara, Y., Wakamori, M., Ishii, M., Maeno, E., Nishida, M., Yoshida, T., Yamada, H., Shimizu, S., Mori, E., Kudoh, J., Shimizu, N., Kurose, H., Okada, Y., Imoto, K., and Mori, Y. (2002) *Mol. Cell* **9**, 163–173
3. Wehage, E., Eisfeld, J., Heiner, I., Jungling, E., Zitt, C., and Luckhoff, A. (2002) *J. Biol. Chem.* **277**, 23150–23156
4. Perraud, A. L., Fleig, A., Dunn, C. A., Bagley, L. A., Launay, P., Schmitz, C., Stokes, A. J., Zhu, Q., Bessman, M. J., Penner, R., Kinet, J. P., and Scharenberg, A. M. (2001) *Nature* **411**, 595–599
5. Shen, B. W., Perraud, A. L., Scharenberg, A., and Stoddard, B. L. (2003) *J. Mol. Biol.* **332**, 385–398
6. Sano, Y., Inamura, K., Miyake, A., Mochizuki, S., Yokoi, H., Matsushime, H., and Furuichi, K. (2001) *Science* **293**, 1327–1330
7. Kuhn, F. J., and Luckhoff, A. (2004) *J. Biol. Chem.* **279**, 46431–46437
8. Perraud, A. L., Takanishi, C. L., Shen, B., Kang, S., Smith, M. K., Schmitz, C., Knowles, H. M., Ferraris, D., Li, W., Zhang, J., Stoddard, B. L., and Scharenberg, A. M. (2005) *J. Biol. Chem.* **280**, 6138–6148
9. Perraud, A. L., Shen, B., Dunn, C. A., Rippe, K., Smith, M. K., Bessman, M. J., Stoddard, B. L., and Scharenberg, A. M. (2003) *J. Biol. Chem.* **278**, 1794–1801
10. Zhang, W., Chu, X., Tong, Q., Cheung, J. Y., Conrad, K., Masker, K., and Miller, B. A. (2003) *J. Biol. Chem.* **278**, 16222–16229
11. Fonfria, E., Marshall, I. C., Benham, C. D., Boyfield, I., Brown, J. D., Hill, K., Hughes, J. P., Skaper, S. D., and McNulty, S. (2004) *Br. J. Pharmacol.* **143**, 186–192
12. Kolisek, M., Beck, A., Fleig, A., and Penner, R. (2005) *Mol. Cell* **18**, 61–69
13. North, B. J., Marshall, B. L., Borra, M. T., Denu, J. M., and Verdin, E. (2003) *Mol. Cell* **11**, 437–444
14. Schwer, B., North, B. J., Frye, R. A., Ott, M., and Verdin, E. (2002) *J. Cell Biol.* **158**, 647–657
15. Tanner, K. G., Landry, J., Sternglanz, R., and Denu, J. M. (2000) *Proc. Natl. Acad. Sci. U. S. A.* **97**, 14178–14182
16. Rafty, L. A., Schmidt, M. T., Perraud, A. L., Scharenberg, A. M., and Denu, J. M. (2002) *J. Biol. Chem.* **277**, 47114–47122
17. Jackson, M. D., and Denu, J. M. (2002) *J. Biol. Chem.* **277**, 18535–18544
18. Borra, M. T., O'Neill, F. J., Jackson, M. D., Marshall, B., Verdin, E., Foltz, K. R., and Denu, J. M. (2002) *J. Biol. Chem.* **277**, 12632–12641
19. Smith, M. A., Herson, P. S., Lee, K., Pinnock, R. D., and Ashford, M. L. (2003) *J. Physiol.* **547**, 417–425
20. Herson, P. S., Lee, K., Pinnock, R. D., Hughes, J., and Ashford, M. L. (1999) *J. Biol. Chem.* **274**, 833–841
21. McHugh, D., Flemming, R., Xu, S. Z., Perraud, A. L., and Beech, D. J. (2003) *J. Biol. Chem.* **278**, 11002–11006
22. Diefenbach, J., and Burkle, A. (2005) *Cell Mol. Life Sci.* **62**, 721–730
23. Rankin, P. W., Jacobson, E. L., Benjamin, R. C., Moss, J., and Jacobson, M. K. (1989) *J. Biol. Chem.* **264**, 4312–4317
24. Blander, G., and Guarente, L. (2004) *Annu. Rev. Biochem.* **73**, 417–435
25. Frye, R. A. (2000) *Biochem. Biophys. Res. Commun.* **273**, 793–798
26. Frye, R. A. (1999) *Biochem. Biophys. Res. Commun.* **260**, 273–279
27. Jackson, M. D., Schmidt, M. T., Oppenheimer, N. J., and Denu, J. M. (2003) *J. Biol. Chem.* **278**, 50985–50998
28. Sauve, A. A., and Schramm, V. L. (2003) *Biochemistry* **42**, 9249–9256
29. Schmidt, M. T., Smith, B. C., Jackson, M. D., and Denu, J. M. (2004) *J. Biol. Chem.* **279**, 40122–40129
30. Tanny, J. C., and Moazed, D. (2001) *Proc. Natl. Acad. Sci. U. S. A.* **98**, 415–420
31. Sauve, A. A., Celic, I., Avalos, J., Deng, H., Boeke, J. D., and Schramm, V. L. (2001) *Biochemistry* **40**, 15456–15463

32. Kraft, R., Grimm, C., Grosse, K., Hoffmann, A., Sauerbruch, S., Kettenmann, H., Schultz, G., and Harteneck, C. (2004) *Am. J. Physiol. Cell Physiol.* **286**, C129–C137
33. Heiner, I., Eisfeld, J., Halaszovich, C. R., Wehage, E., Jungling, E., Zitt, C., and Luckhoff, A. (2003) *Biochem. J.* **371**, 1045–1053
34. Inamura, K., Sano, Y., Mochizuki, S., Yokoi, H., Miyake, A., Nozawa, K., Kitada, C., Matsushime, H., and Furuichi, K. (2003) *J. Membr. Biol.* **191**, 201–207
35. Qian, F., Huang, P., Ma, L., Kuznetsov, A., Tamarina, N., and Philipson, L. H. (2002) *Diabetes* **51**, Suppl. 1, S183–S189
36. Herson, P. S., and Ashford, M. L. (1999) *J. Physiol.* **514**, 47–57
37. Herson, P. S., and Ashford, M. L. (1997) *J. Physiol.* **501**, 59–66
38. Herson, P. S., Dulock, K. A., and Ashford, M. L. (1997) *J. Physiol.* **505**, 65–76
39. Ercan-Fang, N., Gannon, M. C., Rath, V. L., Treadway, J. L., Taylor, M. R., and Nuttall, F. Q. (2002) *Am. J. Physiol. Endocrinol. Metab.* **283**, E29–E37
40. Grubisha, O., Smith, B. C., and Denu, J. M. (2005) *FEBS J.* **272**, 4607–4616
41. Denu, J. M. (2003) *Trends Biochem. Sci.* **28**, 41–48
42. Brunet, A., Sweeney, L. B., Sturgill, J. F., Chua, K. F., Greer, P. L., Lin, Y., Tran, H., Ross, S. E., Mostoslavsky, R., Cohen, H. Y., Hu, L. S., Cheng, H. L., Jedrychowski, M. P., Gygi, S. P., Sinclair, D. A., Alt, F. W., and Greenberg, M. E. (2004) *Science* **303**, 2011–2015
43. Kobayashi, Y., Furukawa-Hibi, Y., Chen, C., Horio, Y., Isobe, K., Ikeda, K., and Motoyama, N. (2005) *Int. J. Mol. Med.* **16**, 237–243
44. Motta, M. C., Divecha, N., Lemieux, M., Kamel, C., Chen, D., Gu, W., Bultsma, Y., McBurney, M., and Guarente, L. (2004) *Cell* **116**, 551–563
45. Yeung, F., Hoberg, J. E., Ramsey, C. S., Keller, M. D., Jones, D. R., Frye, R. A., and Mayo, M. W. (2004) *EMBO J.* **23**, 2369–2380
46. Cohen, H. Y., Miller, C., Bitterman, K. J., Wall, N. R., Hekking, B., Kessler, B., Howitz, K. T., Gorospe, M., de Cabo, R., and Sinclair, D. A. (2004) *Science* **305**, 390–392
47. Luo, J., Nikolaev, A. Y., Imai, S., Chen, D., Su, F., Shiloh, A., Guarente, L., and Gu, W. (2001) *Cell* **107**, 137–148
48. Vaziri, H., Dessain, S. K., Ng Eaton, E., Imai, S. I., Frye, R. A., Pandita, T. K., Guarente, L., and Weinberg, R. A. (2001) *Cell* **107**, 149–159
49. Langley, E., Pearson, M., Faretta, M., Bauer, U. M., Frye, R. A., Minucci, S., Pelicci, P. G., and Kouzarides, T. (2002) *EMBO J.* **21**, 2383–2396
50. van der Horst, A., Tertoolen, L. G., de Vries-Smits, L. M., Frye, R. A., Medema, R. H., and Burgering, B. M. (2004) *J. Biol. Chem.* **279**, 28873–28879
51. Yang, Y., Hou, H., Haller, E. M., Nicosia, S. V., and Bai, W. (2005) *EMBO J.* **24**, 1021–1032
52. Fulco, M., Schiltz, R. L., Iezzi, S., King, M. T., Zhao, P., Kashiwaya, Y., Hoffman, E., Veech, R. L., and Sartorelli, V. (2003) *Mol. Cell* **12**, 51–62
53. Picard, F., Kurtev, M., Chung, N., Topark-Ngarm, A., Senawong, T., Machado De Oliveira, R., Leid, M., McBurney, M. W., and Guarente, L. (2004) *Nature* **429**, 771–776
54. Rodgers, J. T., Lerin, C., Haas, W., Gygi, S. P., Spiegelman, B. M., and Puigserver, P. (2005) *Nature* **434**, 113–118
55. Moynihan, K. A., Grimm, A. A., Plueger, M. M., Bernal-Mizrachi, E., Ford, E., Cras-Meneur, C., Permutt, M. A., and Imai, S. (2005) *Cell Metab.* **2**, 105–117
56. Rose, G., Dato, S., Altomare, K., Bellizzi, D., Garasto, S., Greco, V., Passarino, G., Feraco, E., Mari, V., Barbi, C., BonaFe, M., Franceschi, C., Tan, Q., Boiko, S., Yashin, A. I., and De Benedictis, G. (2003) *Exp. Gerontol.* **38**, 1065–1070
57. Bellizzi, D., Rose, G., Cavalcante, P., Covello, G., Dato, S., De Rango, F., Greco, V., Maggiolini, M., Feraco, E., Mari, V., Franceschi, C., Passarino, G., and De Benedictis, G. (2005) *Genomics* **85**, 258–263
58. Shi, T., Wang, F., Stieren, E., and Tong, Q. (2005) *J. Biol. Chem.* **280**, 13560–13567
59. Kustatscher, G., Hothorn, M., Pugieux, C., Scheffzek, K., and Ladurner, A. G. (2005) *Nat. Struct. Mol. Biol.* **12**, 624–625
60. Liou, G. G., Tanny, J. C., Kruger, R. G., Walz, T., and Moazed, D. (2005) *Cell* **121**, 515–527
61. Berger, F., Ramirez-Hernandez, M. H., and Ziegler, M. (2004) *Trends Biochem. Sci.* **29**, 111–118

Metabolite of SIR2 Reaction Modulates TRPM2 Ion Channel

Olivera Grubisha, Louise A. Rafty, Christina L. Takanishi, Xiaojie Xu, Lei Tong,
Anne-Laure Perraud, Andrew M. Scharenberg and John M. Denu

J. Biol. Chem. 2006, 281:14057-14065.

doi: 10.1074/jbc.M513741200 originally published online March 24, 2006

Access the most updated version of this article at doi: [10.1074/jbc.M513741200](https://doi.org/10.1074/jbc.M513741200)

Alerts:

- [When this article is cited](#)
- [When a correction for this article is posted](#)

[Click here](#) to choose from all of JBC's e-mail alerts

This article cites 61 references, 25 of which can be accessed free at
<http://www.jbc.org/content/281/20/14057.full.html#ref-list-1>